

# Letters

## *The formation of $\alpha'$ lath martensite in a textured ( $\alpha + \gamma$ ) Fe-23.19 wt % Cr-4.91 wt % Ni alloy*

It is known that the rate of martensite transformation during tensile straining is dependent upon the direction of the applied stress [1], and that the formation of martensite from textured austenite ( $\gamma$ ) is affected by the stress axis [2]. The integrated intensity of the  $(211)_M$  reflection for tensile directions at  $0^\circ$  and  $45^\circ$  to the rolling direction was greater than those of the  $(200)_M$  and  $(110)_M$  reflections, while the integrated intensity ratios of  $(200)_M$  and  $(110)_M$  reflections in a  $90^\circ$  specimen were greater than that of  $(211)_M$  [3]. The subscript M refers to a plane of bcc martensite or ferrite. In fractured specimens with tensile directions at  $0^\circ$ ,  $45^\circ$  and  $90^\circ$  to the rolling direction, it has been shown that the different integrated intensity ratios occur due to the formation of particular Kurdjumov-Sachs (K-S), variants during martensite transformation [4]. In the present study, this particular formation of  $\alpha'$  laths is discussed.

The composition (wt%) of the two-phase Fe-Cr-Ni alloy, with ferrite ( $\alpha$ ) and austenite ( $\gamma$ ) phases, used in the present work, was 23.19 Cr, 4.91 Ni, 0.025 C, 1.47 Mo, 0.53 Si, 0.51 Mn, 0.91 Al, 0.023 P, with the balance Fe. Sheet specimens 2.0 mm thick were cut parallel to the rolling direction, to make a gauge section 6.0 mm  $\times$  18.0 mm. The sheet specimens were annealed for 1 h at 1273 K in a vacuum furnace, to produce an alloy with a mean grain diameter of 8.0  $\mu$ m and containing 52 vol% of  $\gamma$ . The resultant  $(200)_A$  pole figure of the  $\gamma$  phase contained both  $(110)_A$   $[\bar{3}32]_A$  and  $(225)_A$   $[\bar{2}\bar{3}2]_A$  components, as shown in Fig. 1. The subscript A refers to a plane of austenite. The specimens were deformed to tensile strains of 4, 18, 28, 32 and 38% at 77 K, in an Instron-type testing machine at a cross-head speed of  $0.8 \times 10^{-5}$  msec $^{-1}$ . After tensile deformation, six X-ray diffraction patterns of  $(111)_A$ ,  $(200)_A$  and  $(220)_A$  reflections, and  $(110)_M$ ,  $(200)_M$  and  $(211)_M$  reflections were measured to determine the presence of  $\alpha'$  lath martensite induced by tensile straining.

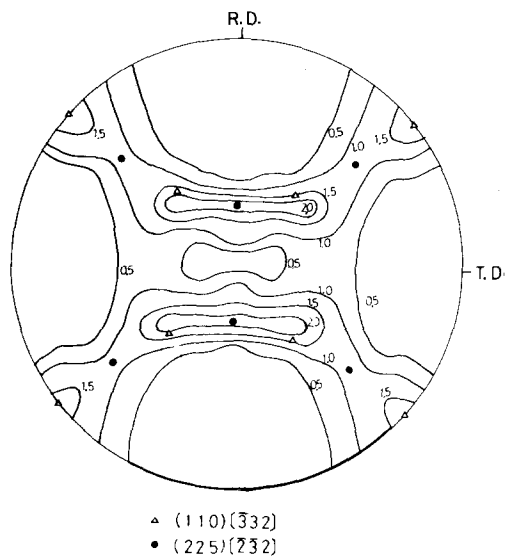


Figure 1  $(200)_A$  pole figure. The triangle indicates a  $(110)_A$   $[\bar{3}32]_A$  component and the closed circle a  $(225)_A$   $[\bar{2}\bar{3}2]_A$  component. R. D. and T. D. indicate rolling and transverse directions, respectively

Fig. 2 shows the variation of the integrated intensity ratio with tensile strain at 77 K. The ratios for the  $(111)_A$ ,  $(200)_A$ ,  $(220)_A$ ,  $(110)_M$ ,  $(200)_M$  and  $(211)_M$  reflections are the ratios of integrated intensity for a specimen deformed to a certain tensile strain,  $I$ , to those of an annealed specimen,  $I^0$ . The ratios for the  $(111)_A$ ,  $(200)_A$  and  $(220)_A$  reflections decreased with increasing tensile strain due to the occurrence of martensite transformation, and reached a zero value at 38.0% strain, at which all the  $\gamma$  transformed to  $\alpha'$ . In contrast the integrated intensity ratios for the  $(211)_M$ ,  $(200)_M$  and  $(110)_M$  reflections changed to  $\sim 2.5$ , 1.3 and 0.7, respectively, at this tensile strain. It is therefore deduced that there are more  $(211)_M$  reflections than  $(200)_M$  and  $(110)_M$  reflections.

Table I shows the values of  $U/\sigma$  in 24 K-S variants for the  $[323]_A$  and  $[223]_A$  tensile axes in the  $\{111\}_A$   $\langle 112 \rangle_A$  shear system.  $U$  and  $\sigma$  are the work done by the martensite transformation due to the action of applied stress and the applied stress, respectively. Thus,  $U/\sigma$  indicates the mech-

TABLE I Values of  $U/\sigma$  in 24 K-S variants for  $[3\ 2\ 3]_A$  and  $[2\ 2\ 3]_A$  tensile axes

K-S relation		Variant notation	Values of $U/\sigma$ in two tensile directions	
Plane (A)    (M)	Direction [A]    [M]		$[3\ 2\ 3]$	$[2\ 2\ 3]$
$(\bar{1}\ \bar{1}\ \bar{1}) \parallel (1\ 1\ 0)$	$[\bar{1}\ 0\ \bar{1}]$ $[\bar{1}\ \bar{1}\ \bar{1}]$	-1	0.0624	0.0426
	$[0\ \bar{1}\ \bar{1}]$ $[\bar{1}\ \bar{1}\ 1]$	-2	0.0779	0.0214
	$[\bar{1}\ \bar{1}\ 0]$ $[\bar{1}\ \bar{1}\ \bar{1}]$	1-3	0.0779	0.1115
	$[\bar{1}\ 0\ 1]$ $[\bar{1}\ \bar{1}\ 1]$	-4	0.0624	0.1019
	$[0\ 1\ 1]$ $[\bar{1}\ \bar{1}\ \bar{1}]$	-5	-0.0455	-0.0424
	$[1\ 1\ 0]$ $[\bar{1}\ \bar{1}\ 1]$	-6	-0.0455	-0.0467
$(1\ 1\ 1) \parallel (1\ 1\ 0)$	$[\bar{1}\ 0\ 1]$ $[\bar{1}\ \bar{1}\ \bar{1}]$	-1	-0.0024	-0.0025
	$[\bar{1}\ 0\ \bar{1}]$ $[\bar{1}\ \bar{1}\ 1]$	-2	0.0032	-0.0025
	$[1\ \bar{1}\ 0]$ $[\bar{1}\ \bar{1}\ \bar{1}]$	2-3	0.0032	0.0035
	$[1\ 0\ \bar{1}]$ $[\bar{1}\ \bar{1}\ 1]$	-4	-0.0024	0.0100
	$[0\ 1\ \bar{1}]$ $[\bar{1}\ \bar{1}\ \bar{1}]$	-5	0.0036	0.0100
	$[\bar{1}\ 1\ 0]$ $[\bar{1}\ \bar{1}\ 1]$	-6	0.0036	0.0035
$(1\ \bar{1}\ \bar{1}) \parallel (1\ 1\ 0)$	$[\bar{1}\ 0\ \bar{1}]$ $[\bar{1}\ \bar{1}\ \bar{1}]$	-1	0.0717	0.0214
	$[0\ 1\ \bar{1}]$ $[\bar{1}\ \bar{1}\ 1]$	-2	0.0547	0.0426
	$[1\ 1\ 0]$ $[\bar{1}\ \bar{1}\ \bar{1}]$	3-3	-0.0554	-0.0467
	$[1\ 0\ 1]$ $[\bar{1}\ \bar{1}\ 1]$	-4	-0.0499	-0.0424
	$[0\ \bar{1}\ 1]$ $[\bar{1}\ \bar{1}\ \bar{1}]$	-5	0.1104	0.1019
	$[\bar{1}\ \bar{1}\ 0]$ $[\bar{1}\ \bar{1}\ 1]$	-6	0.1234	0.1115
$(\bar{1}\ \bar{1}\ 1) \parallel (1\ 1\ 0)$	$[1\ 0\ 1]$ $[\bar{1}\ \bar{1}\ \bar{1}]$	-1	-0.0499	-0.0564
	$[0\ 1\ 1]$ $[\bar{1}\ \bar{1}\ 1]$	-2	-0.0554	-0.0564
	$[\bar{1}\ 1\ 0]$ $[\bar{1}\ \bar{1}\ \bar{1}]$	4-3	0.0547	0.0873
	$[\bar{1}\ 0\ \bar{1}]$ $[\bar{1}\ \bar{1}\ 1]$	-4	0.0717	0.1046
	$[0\ \bar{1}\ \bar{1}]$ $[\bar{1}\ \bar{1}\ \bar{1}]$	-5	0.1234	0.1046
	$[\bar{1}\ \bar{1}\ 0]$ $[\bar{1}\ \bar{1}\ 1]$	-6	0.1104	0.0873

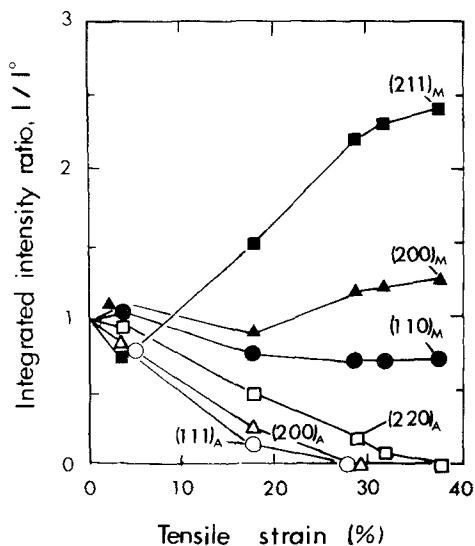


Figure 2 The variation of integrated intensity ratio of  $(211)_M$ ,  $(200)_M$ ,  $(110)_M$ ,  $(220)_A$ ,  $(200)_A$  and  $(111)_A$  reflections with tensile strain at 77 K.

anical work per unit volume of austenite reacted to martensite, as defined by Patel and Cohen [5].

In the shear system, the habit plane and the direction of shape deformation were assumed to be  $\{1\ 1\ 2\}_A$  and  $\langle 1\ 1\ 0 \rangle_A$ , respectively, according to the stereographic projection shown in [4]. The values of  $U/\sigma$  had either plus or minus signs, as shown in Table I. K-S variants with plus and minus signs form by tensile straining and compression testing, respectively [6]. As tensile deformation is carried out, it is expected that the K-S variants with the maximum value of  $U/\sigma$  are induced by the deformation. Thus, 3-6 and 4-5 variants; and 1-3 and 3-6 variants were detected for the  $[3\ 2\ 3]_A$  and  $[2\ 2\ 3]_A$  tensile axes, respectively. In [4], 3-6 in  $[3\ 2\ 3]_A$  and 1-3 in  $[2\ 2\ 3]_A$  are K-S variants which form the  $\{2\ 1\ 1\}_M$  poles.

In the present study the double shear process, proposed by Bogers and Burgers [7], is discussed to obtain possible K-S variants in relation to the process, as suggested by Higo *et al.* [8]. Table II

TABLE II Values of Schmid factor in 12 shear directions for  $[3\ 2\ 3]_A$  and  $[2\ 2\ 3]_A$  tensile axes

Plane (A)	Shear direction [A]	Thompson tetrahedron notation	Values of Schmid factor in two tensile directions	
			$[3\ 2\ 3]$	$[2\ 2\ 3]$
$(\bar{1}\ 1\ \bar{1})$	$[2\ 1\ \bar{1}]$	$C\alpha$	-0.204	-0.124
	$[\bar{1}\ \bar{2}\ \bar{1}]$	$D\alpha$	0.421	0.365
	$[\bar{1}\ 1\ 2]$	$B\alpha$	-0.217	-0.240
(1 1 1)	$[\bar{2}\ 1\ 1]$	$B\delta$	-0.066	-0.100
	$[1\ \bar{2}\ 1]$	$A\delta$	0.159	0.081
	$[1\ 1\ \bar{2}]$	$C\delta$	-0.093	-0.181
$(1\ \bar{1}\ \bar{1})$	$[2\ \bar{1}\ \bar{1}]$	$D\beta$	0.253	0.378
	$[1\ 2\ \bar{1}]$	$C\beta$	-0.093	-0.133
	$[\bar{1}\ 1\ 2]$	$A\beta$	-0.161	-0.246
$(\bar{1}\ \bar{1}\ 1)$	$[2\ \bar{1}\ 1]$	$A\gamma$	-0.143	-0.075
	$[\bar{1}\ 2\ 1]$	$B\gamma$	-0.088	-0.077
	$[\bar{1}\ \bar{1}\ \bar{2}]$	$D\gamma$	0.231	0.152

shows the values of Schmid factor in 12 shear directions for  $[3\ 2\ 3]_A$  and  $[2\ 2\ 3]_A$  tensile axes. As a shear direction with a maximum value of Schmid factor,  $D\alpha$  and  $D\beta$  are found for  $[3\ 2\ 3]_A$  and  $[2\ 2\ 3]_A$  tensile axes, respectively. In  $[3\ 2\ 3]_A$  tensile axis, 1-5 and 1-6 variants contain  $D\alpha$  as a first shear and 3-6 and 4-4 contain  $D\beta$  as a second shear and 3-3 and 3-4 contain  $D\beta$  as a first shear in  $[2\ 2\ 3]_A$  axis. As shown in Table I, 1-5 and 1-6 variants in  $[3\ 2\ 3]_A$  and 3-3 and 3-4 variants in  $[2\ 2\ 3]_A$ , are formed by compression testing, and 4-4 variants in  $[2\ 2\ 3]_A$  have the second largest value of  $U/\sigma$ . K-S variants obtained by Schmid factor do not necessary agree with those which are obtained by the  $U/\sigma$  calculation. Then, by discussing K-S variants obtained from two methods, 3-6 variant in  $[3\ 2\ 3]_A$

and 1-3 variant in  $[2\ 2\ 3]_A$  are selected as the variants which agree each other. Finally, calculating both the interaction of applied stress with displacive shear during martensite transformation and possible Kurdjumov-Sachs variants in relation to the double shear process, Kurdjumov-Sachs variants induced by tensile deformation were obtained (Table II).

## References

1. R. LAGNEBORG, *Acta Met.* 12 (1964) 823.
2. D. GOODCHILD, W. T. ROBERTS and D. V. WILSON, *ibid.* 18 (1970) 1137.
3. T. NAKAMURA and K. WAKASA, *Scripta Met.* 9 (1975) 959.
4. K. WAKASA and T. NAKAMURA, *J. Mater. Sci.* 13 (1978) 21.
5. J. R. PATEL and M. COHEN, *Acta Met.* 1 (1953) 531.
6. M. KATO and T. MORI, *ibid.* 24 (1976) 853.
7. A. J. BOGERS and W. G. BURGERS, *ibid.* 12 (1964) 225.
8. Y. HIGO, F. LECROISEY and T. MORI, *ibid.* 22 (1974) 313.

Received 22 December 1977  
and accepted 10 March 1978.

KUNIO WAKASA\*  
Institute for Medical and Dental Engineering,  
Tokyo Medical and Dental University,  
2-3-10 Surugadai,  
Kanda, Chiyoda-ku,  
Tokyo, Japan  
TADAHISA NAKAMURA  
Department of Materials Science and Engineering,  
Tokyo Institute of Technology,  
O-okayama, Meguro-ku,  
Tokyo, Japan

\*Now at: Department of Metallurgy and Mining Engineering, University of Illinois at Urbana, Champaign, Urbana, Illinois 61801, USA.

## Explosive-shock deformation of natural chalcopyrite ( $CuFeS_2$ )

The authors recently described the defect structure in natural chalcopyrite utilizing transmission electron microscopy [1]. On the basis of these observations, it was concluded that the apparently low stacking-fault free energy in  $CuFeS_2$  which was deduced from numerous observations of

stacking faults, would give rise to abundant mechanical twins accommodating large deformations. It was assumed in fact, that large numbers of stacking faults and twin faults might form in response to large deformation such as explosive-shock deformation as in the case of fcc metals and alloys and other minerals [2-5].

The present study involved an experiment to test this prediction. A whole section of natural